Incorporating the BEST Methodology in Experiments for Measuring Paramagnetic Relaxation Enhancements

Nikolaus M. Loening[1]
[1]Department of Chemistry, Lewis & Clark College, Portland, Oregon, United States.

Abstract

Band-selective excitation short-transient (BEST) sequences are widely used for protein NMR experiments that start with amide proton magnetization, such as ^{1}H-^{15}N HSQC, ^{1}H-^{15}N TROSY, and multidimensional backbone assignment experiments, because the optimization of amide proton longitudinal relaxation afforded by the BEST methodology allows for much greater sensitivity when using short scan times. Here we show that the BEST methodology can be easily incorporated in sequences for measuring proton transverse relaxation rates (^{1}H R_2), which are typically used to determine paramagnetic relaxation enhancements (PREs). The resulting BEST-HSQC-PRE and BEST-TROSY-PRE experiments afford similar or better sensitivity for measuring PREs compared to previous methods, provide equally accurate measurements of transverse relaxation rates (and therefore PREs), and allow shorter scan times to be used.

Keywords

Paramagnetic relaxation enhancement, BEST, HSQC, TROSY, transverse relaxation

Introduction

Paramagnetic relaxation enhancements (PREs) are a powerful tool for obtaining long-range distance constraints in NMR spectroscopy, and are particularly useful for probing dark states, measuring transient interactions in intrinsically disordered proteins and protein complexes, and as a complement to measurements of the nuclear Overhauser effect[1–5]. In theory, longitudinal or transverse relaxation rates for any nucleus can be used for measuring PREs. However, for a variety of practical purposes, proton (^{1}H) transverse relaxation rates are best suited for accurate PRE measurements due to the high gyromagnetic ratio and sensitivity of ^{1}H and because transverse relaxation is less susceptible to fast-internal motion, cross-relaxation, and hydrogen exchange with the solvent than longitudinal relaxation[5]. Determining PREs for protein samples typically involves acquiring two ^{1}H-^{15}N correlation pseudo-3D experiments for determining ^{1}H R_2 values: one for when the sample has a paramagnetic label and a second control experiment after the label has been reduced to a diamagnetic state. The difference between the relaxation rates measured in the two experiments is the PRE (Γ_2):

$$\Gamma_2 = R_{2,\text{paramagnetic}} - R_{2,\text{diamagnetic}} \quad (1)$$

Longitudinal relaxation-optimized pulse sequences are widely used for protein NMR experiments as they allow faster repetition rates and better sensitivity[6–9]. They work by leaving non-amide protons along the longitudinal axis at (or near) thermal equilibrium at the end of each repetition of a pulse sequence. This pool of protons interacts with the amide protons to increase the effective longitudinal relaxation rates of the amide protons. As a consequence, the recycle delay that results in the best sensitivity (signal-to-noise per unit time) is greatly reduced for protein NMR experiments that start with amide proton magnetization, such as ^{1}H-^{15}N HSQC, ^{1}H-^{15}N TROSY, and multidimensional backbone assignment experiments. The relaxation optimization effect is increased for larger proteins and at higher magnetic fields, but even for small proteins at moderate fields sensitivity is usually increased and, more importantly, more increments of a multi-dimensional experiment can be collected in a given amount of experiment time without sacrificing sensitivity. Band-selective excitation short-transient (BEST) sequences[9–13] are a category of longitudinal

relaxation-optimized experiments which, as the name implies, use band-selective pulses to selectively excite amide protons while leaving other protons unperturbed.

Here we show that the BEST methodology can be easily incorporated into pseudo-3D sequences used for determining ^{1}H R_2 values and, consequently, PREs. The resulting BEST-HSQC-PRE and BEST-TROSY-PRE experiments afford similar or better sensitivity for measuring ^{1}H R_2 values compared to non-BEST methods, have similar accuracy, and allow shorter scan times to be used. In the following, we refer to the pulse sequences for measuring ^{1}H R_2 values as "PRE" experiments, as the resulting ^{1}H R_2 values are most frequently used to measure PREs and rarely used for anything else.

Materials and Methods

Sample Preparation

All experiments were carried out using ^{15}N-labeled samples of a N-terminal construct of *Rattus norvegicus* dynein intermediate chain (IC-2C$_{1\text{-}96}$). The expression and purification of this protein has been previously described[14]. Briefly, expression was carried out using ^{15}N-labeled MJ9 minimal media cultures[15] that were used to grow *Escherichia coli* containing a pET-24 plasmid coding for His-tagged IC-2C$_{1\text{-}96}$. After induction and further growth, the cultures were pelleted, lysed by sonication, and clarified by high-speed centrifugation. The clarified lysates were purified using immobilized metal affinity chromatography (IMAC), cleaved with His-tagged TEV protease[16], and then purified again using a second IMAC step to separate cleaved IC-2C$_{1\text{-}96}$ from the His tag, His-tagged TEV protease, and metal-binding bacterial protein impurities. Size-exclusion chromatography (SEC) was then used as a final purification step. The purity of the samples was verified by sodium dodecyl sulfate–polyacrylamide gel electrophoresis (SDS-PAGE) analysis to be greater than 95%, and protein concentrations were determined by measuring the absorbance at 205 nm[17] as IC-2C$_{1\text{-}96}$ does not have residues (tyrosine and tryptophan) that absorb at 280 nm.

NMR measurements and analysis

For NMR spectroscopy, samples of ^{15}N-labeled IC-2C$_{1\text{-}96}$ at a concentration of 600 μM were prepared in a 150 mM sodium chloride, 50 mM phosphate (pH 7.4) buffer that included 5% D_2O and 0.2 mM 2,2-dimethylsilapentane-5-sulfonic acid (DSS), and then loaded into reduced-volume (Shigemi) 5 mm NMR tubes. NMR spectra were collected at 10ºC using an Avance NEO 600 MHz spectrometer (Bruker BioSpin) equipped with a room-temperature TXI probe. Some experiments were also carried out using a room-temperature TBO probe.

NMR data were processed using TopSpin 4.5 (Bruker BioSpin). Peak assignment was performed using CCPN Analysis 2.5.2[18]. Peak heights were determined using a parabolic fit, and the change in peak height with increasing delay time for each peak was then fit to an exponential function ($A \exp(-Bx)$) with errors estimated using a covariance method.

All pseudo-3D experiments (HSQC-PRE, BEST-HSQC-PRE, TROSY-PRE, and BEST-TROSY-PRE) were carried out with 160 increments in the indirect (^{15}N) dimension, 16 scans per increment, and eight different variable delay times (Δ) in the pseudo-dimension (0, 2.5, 5, 10, 15, 20, 25, and 30 ms). Including an acquisition time of 87 ms and a disk input/output time of 30 ms, the time required for each scan was approximately 140 ms (when $\Delta = 0$ and $t_1 = 0$) for the HSQC-PRE and TROSY-PRE experiments, and approximately 150 ms (when $\Delta = 0$ and $t_1 = 0$) for the BEST-HSQC-PRE and BEST-TROSY-PRE experiments. For comparing the influence of the recycle delay on the experimental results, recycle delays of 0.2, 0.5, 1.0, 2.0, and 4.0 seconds were used while keeping all other parameters (such as the number of increments and the number of scans per increment) constant, resulting in experiment times of approximately 2.1, 3.9, 6.8, 12.4, and 23.7 h, respectively.

Results

The HSQC-PRE experiment shown at the top of Fig. 1 is a "conventional" HSQC-based ^{1}H R_2 measurement sequence that is closely based on a sequence proposed by Donaldson et al.[19]. The main difference is that the HSQC-PRE sequence shown in Fig. 1 uses a preservation of equivalent pathways (PEP) scheme for the reverse INEPT step to provide sensitivity enhancement[20,21]. In all the sequences in Fig. 1, a variable delay (Δ) during the first coherence transfer step is increased between increments to add an exponential weighting to the signal (S) that depends on the transverse relaxation rate:

$$S = S_0 \, e^{-R_2 \Delta} \tag{2}$$

where S_0 is the signal when $\Delta = 0$. A band-selective 180º pulse is used in the first INEPT transfer to refocus couplings between the amide and aliphatic protons. If a hard 180º pulse is used instead, as has been proposed by Iwahara et al.[22], relaxation losses are slightly less, resulting in slightly higher signal-to-noise, but the signal decay will be modulated by the coupling between the amide proton and the alpha proton ($^3J_{H_NH_\alpha}$). This modulation results in a systematic error that affects measurements of $R_{2,\text{paramagnetic}}$ and $R_{2,\text{diamagnetic}}$ equally such that PRE values (Γ_2) calculated using Eq. 1 are still correct even though the individual measurements of R_2 rates will be artificially large. Similarly, the use of a spin echo in these pulse sequences rather than a Carr-Purcell-Meiboom-Gill (CPMG) sequence[23] for the incremented delay time (Δ) simplifies the pulse sequences but potentially reduces the accuracy of the measured ^{1}H R_2 values. For PRE measurements, this potential systematic error will affect $R_{2,\text{paramagnetic}}$ and $R_{2,\text{diamagnetic}}$ equally and therefore will be canceled out when Γ_2 is calculated using Eq. 1.

Our BEST-HSQC-PRE experiment shown in Fig. 1 replaces all hard pulses on the ^{1}H channel with a combination of band-selective pulses that only affect amide protons and a pair of broadband inversion pulses (BIP) that have the net effect of returning solvent and aliphatic protons to their equilibrium positions. The use of band-selective pulses enhances the longitudinal relaxation of the amide protons during the recycle delay because both aliphatic and solvent protons have been left in their equilibrium position. The result is that amide protons return to equilibrium much more rapidly, thereby allowing the recycle delay between scans to be reduced. Shown at the bottom of Fig. 1 are our transverse relaxation-optimized spectroscopy (TROSY[24]) versions of the "conventional" and BEST ^{1}H R_2 measurement experiments. These substitute a double spin-state-selective coherence transfer (S3CT) block[25] for the reverse INEPT step to select for the slowly relaxing components of the ^{1}H-^{15}N doublet.

All sequences in Fig. 1 include an initial ^{15}N excitation pulse followed by a homospoil gradient to disperse any residual ^{15}N magnetization. In addition, a two-step phase cycle is used for the first ^{1}H pulse. This ensure that all magnetization observed at the end of the experiment originates with this pulse and therefore it all is attenuated by ^{1}H R_2 during the incremented Δ delay to the same extent. For the BEST-TROSY-PRE and TROSY-PRE experiments the homospoil and two-step phase cycle decreases the sensitivity of these experiments compared to the regular 2D BEST-TROSY and TROSY experiments because this prevents the simultaneous exploitation of ^{1}H and ^{15}N magnetization[13]. However, the additional ^{15}N magnetization would not be modulated in the same way as the ^{1}H magnetization by the incremented delay (Δ) and therefore needs to be excluded in the BEST-TROSY-PRE and TROSY-PRE experiments to accurately measure ^{1}H R_2.

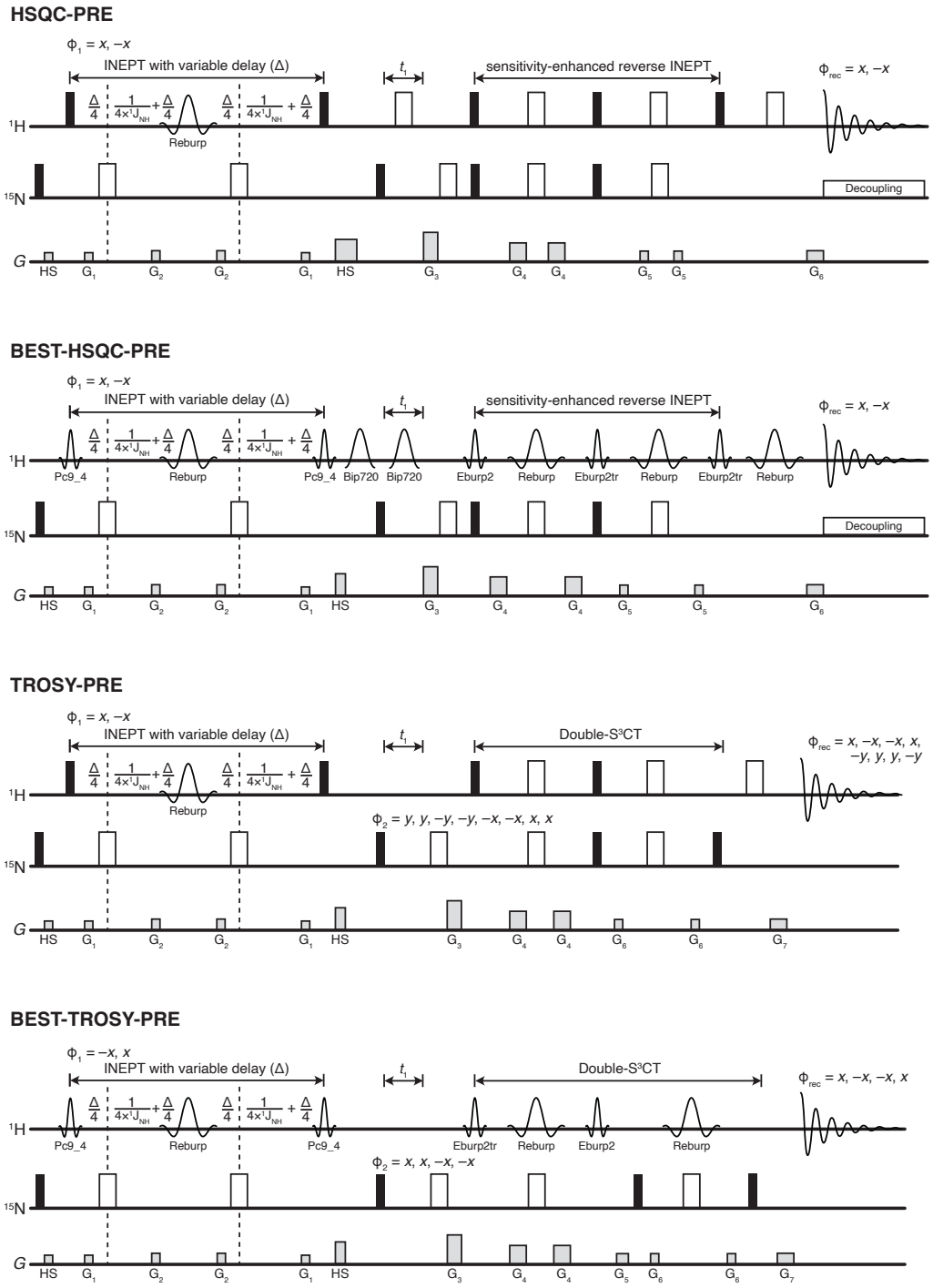

Figure 1: Pseudo-3D experiments for measuring ^{1}H transverse relaxation rates (^{1}H R_2). The HSQC-PRE sequence shown at top is a sensitivity-enhanced HSQC experiment with a variable delay (Δ) during the first INEPT period to generate a pseudo-third dimension with ^{1}H R_2 weighting. The band-selective 180° pulse refocuses H_N-H_α couplings that otherwise cause the measured R_2 values to be artificially large. Below it is the BEST-HSQC-PRE version of the sequence. The TROSY equivalents of the HSQC and BEST-HSQC-PRE experiments are shown at bottom. The initial pulse on ^{15}N followed by a homospoil gradient is to disperse any residual ^{15}N magnetization. When using short recycle delays, a two-step phase cycle is used for the first ^{1}H pulse to subtract out additional magnetization that otherwise builds up with increasing Δ values and affects the accuracy of the resulting ^{1}H R_2 values.

Representative data from a BEST-HSQC-PRE experiment for a ^{15}N-labeled IC-2C$_{1\text{-}96}$ sample are shown in Fig. 2. Each pseudo-3D transverse relaxation measurement experiment consists of a series of 2D ^{1}H-^{15}N planes corresponding to different values of the variable delay Δ. As shown on the right of Fig. 2, peak heights for three representative amide residues decay exponentially and can be fit to Eq. 2 to extract the ^{1}H R_2 value for each amide proton. The ^{1}H R_2 values for these three residues determined using data from the BEST-HSQC-PRE experiment or the more conventional HSQC-PRE experiment (acquired using roughly three times as much experiment time) are within experimental error of each other.

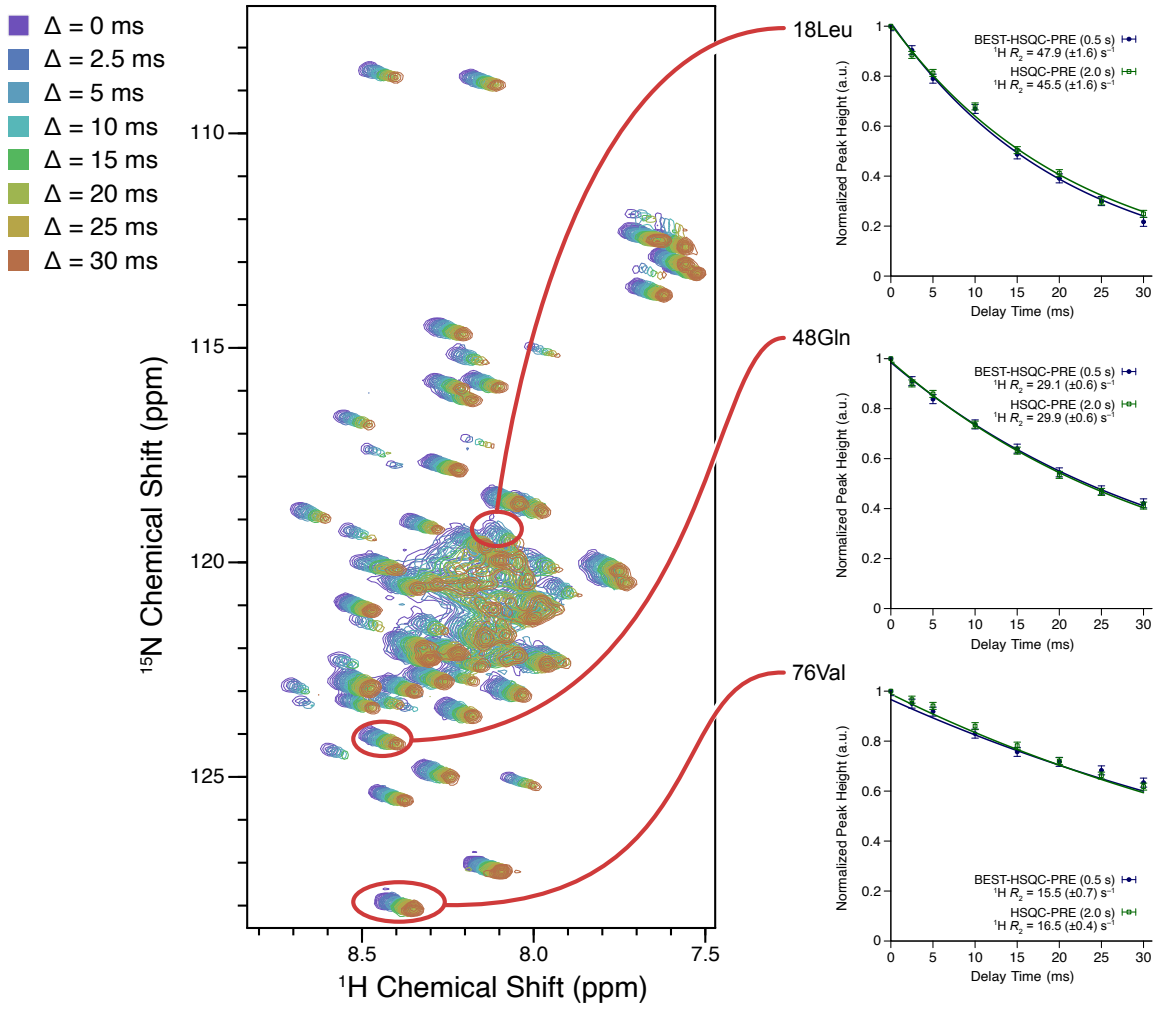

Figure 2: BEST-HSQC-PRE experiments result in identical measurements of ^{1}H R_2 to those determined using HSQC-PRE experiments. Shown at left is a pseudo-3D data set with eight values of Δ in the pseudo-dimension acquired using the BEST-HSQC-PRE experiment and a 600 μM ^{15}N-labeled IC-2C$_{1\text{-}96}$ sample at 10°C with a recycle delay of 0.5 s on a 600 MHz spectrometer; the total experiment time was four hours. Spectra for different values of Δ are offset to better illustrate the decrease in peak intensities with increasing Δ values. The decay curves for individual peaks in the spectrum at right show how the data are fit to exponential functions (Eq. 2) to determine ^{1}H R_2 values, and show that equivalent ^{1}H R_2 values are measured using a BEST-HSQC-PRE experiment with a relatively short recycle delay (0.5 s, total experiment time 4 h) and a HSQC-PRE experiment with a relatively long recycle delay (2.0 s, total experiment time 12 h).

Due to the more rapid return toward equilibrium of amide protons during the recycle delay in BEST experiments, the optimal recycle delay for BEST-PRE experiments is much shorter than for regular PRE experiments. Fig. 3A shows sensitivity (signal-to-noise per unit time) versus scan time (i.e., the sum of the pulse sequence length, the acquisition time, and the recycle delay). For our sample conditions, the BEST-HSQC-PRE and BEST-TROSY-PRE sequences had optimal sensitivity when the total scan time was around 0.5 s (corresponding to a recycle delay of ~0.4 s), whereas the non-BEST versions had optimal sensitivity with scan times of ~1.5 s. What this means is that for a given amount of experiment time the ideal signal-to-noise is achieved by running more scans with a shorter recycle delay for the BEST experiments and running fewer scans with a longer recycle delay for the non-BEST ("conventional") experiments. The higher sensitivity at the optimal scan time for the BEST experiments compared to their non-BEST counterparts (at their optimal scan times) shows that the BEST experiments will result in better signal-to-noise for this particular sample if the optimal recycle delays are used.

Fig. 3B and 3C compare ^{1}H R_2 values determined from BEST-HSQC-PRE and BEST-TROSY-PRE experiments to values determined from HSQC-PRE and TROSY-PRE experiments. These graphs compare BEST sequences taken with the shortest recycle delay used (0.2 s corresponding to a 0.35 s scan time) to non-BEST sequences taken with the longest recycle delay used (4.0 s corresponding to a 4.14 s scan time). These recycle delays are not optimal for getting the best sensitivity within a set amount of experimental time, but were instead chosen to highlight that the BEST results taken with the shortest recycle delays compare well to non-BEST results under conditions where the amide protons are able to almost fully relax between each scan. The error bars for the results from the BEST sequences are generally larger than those from the non-BEST sequences because the same total number of scans were used in each experiment. Consequently, the BEST experiments had worse signal-to-noise because they were acquired in only 2.1 hrs, whereas almost 12 times as much time was used to collect the data for the non-BEST experiments. When comparing experiments for recycle delays with similar sensitives, the errors are similar for BEST and non-BEST experiments (data not shown).

Comparison of results from HSQC-based experiments to TROSY-based experiments (Fig. 3D, BEST-HSQC-PRE vs. BEST-TROSY-PRE and Fig 3E, HSQC-PRE vs. TROSY-PRE) showed linear correlations, which is not surprising as the initial part of these sequences that generates the relaxation weighting is the same in each comparison. As each experiment used the same total number of scans, rather than the same total experiment time, the error bars for values measured using experiments with shorter recycle delays (which were acquired in less experiment time and therefore had worse signal-to-noise ratios) are generally larger than those for experiments with longer recycle delays.

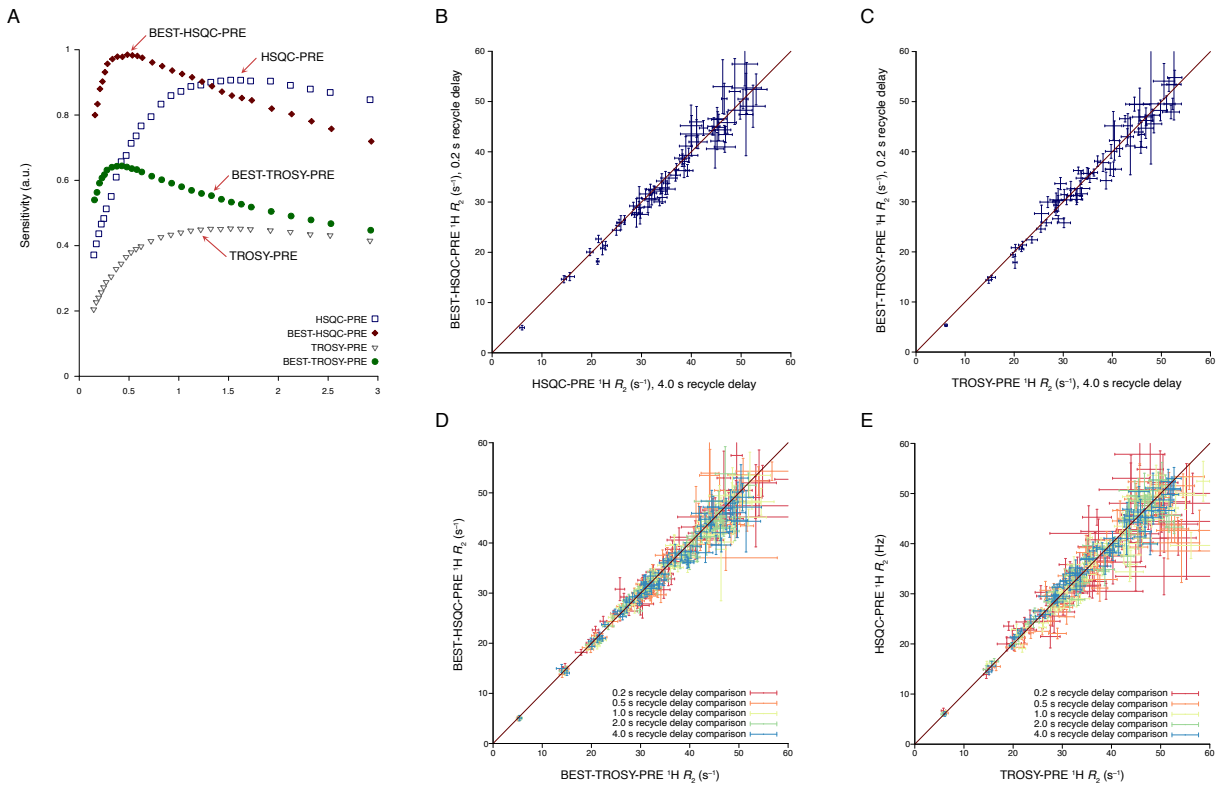

Figure 3: BEST experiments have better sensitivity when optimal scan times are used, have better sensitivity at shorter scan times, and result in equivalent ^{1}H R_2 values compared to non-BEST experiments. (A) Sensitivity for the BEST-HSQC-PRE and BEST-TROSY-PRE experiments is optimal with a scan time of around 0.5 s, whereas the optimal scan time for the HSQC-PRE and TROSY-PRE experiments is around 1.3 s. The sensitivity is calculated as the integral of all backbone amide peaks divided by the square root of the scan time. (B) ^{1}H R_2 values measured using a BEST-HSQC-PRE experiment with a scan time of 0.35 s (recycle delay of 0.2 s, total experiment time of 2.1 h) are within error of those measured using a HSQC-PRE experiment with a scan time of 4.14 s (recycle delay of 4.0 s, total experiment time of 23.7 h). (C) ^{1}H R_2 values measured using a BEST-TROSY-PRE experiment with a scan time of 0.35 s (recycle delay of 0.2 s, total experiment time of 2.1 h) are within error of those measured using a TROSY-PRE experiment with a scan time of 4.14 s (recycle delay of 4.0 s, total experiment time of 23.7 h). (D) Comparison of BEST-HSQC-PRE results to HSQC-PRE results for various recycle delays. (E) Comparison of BEST-TROSY-PRE results to HSQC-TROSY results for various recycle delays. (A-E) All experiments were carried out at 10ºC using a 600 µM ^{15}N-labeled IC-2C$_{1\text{-}96}$ sample on a 600 MHz spectrometer.

Discussion

The relaxation characteristics of the protein being studied will dictate what recycle delay to use, whether to use HSQC or TROSY-based sequences, whether to use sensitivity enhancement for the reverse INEPT step, and whether to use BEST experiments or conventional ones. For the HSQC-based experiments, the PEP scheme for sensitivity enhancement in the reverse INEPT step increases the time spent in the transverse plane and therefore can become counter-productive for rapidly relaxing samples. For both the HSQC- and TROSY-based experiments, the BEST experiments are somewhat longer than the conventional experiments (roughly 30% longer in our case) due to their many band-selective pulses. Fortunately, the time that magnetization spends in the transverse plane is equivalent between BEST and conventional experiments[12],

so the additional time in the BEST experiments predominantly results in some additional longitudinal relaxation which will be much slower than transverse relaxation.

Fortunately, all of these considerations are ones that spectroscopists will have already encountered for each particular protein sample in setting up 2D HSQC or TROSY experiments to check the quality of their samples and in setting up multidimensional experiments for assigning the backbone resonances. The transverse relaxation measurement experiments shown in Fig. 1 are, for the most part, regular HSQC, BEST-HSQC, TROSY, and BEST-TROSY experiments with only the small addition of a variable delay time in the first INEPT step, so the choice of which of these experiments to use will typically follow what was found to be optimal at earlier stages of studying a particular protein sample by NMR spectroscopy. In this paper, the protein used to test the pulse sequences (IC-2$C_{1\text{-}96}$) contains both α-helical (residues 4-38, 52-66) and disordered (the remainder of the protein) regions[26]. Due to the large hydrodynamic radius conferred by the disordered regions, the α-helical regions tumble as if they were in a protein with a much larger molecular weight. This makes the choice of experiment (HSQC versus TROSY) difficult in our case, as on our 600 MHz spectrometer the BEST-HSQC-PRE experiment provides better sensitivity for the dynamic and slowly-relaxing disordered regions whereas the BEST-TROSY-PRE experiment provides better sensitivity for the faster-relaxing α-helical regions. For the decay curves highlighted in Fig. 2, the signal is 50% better for 26Lys and 10% lower for 47Gln and 76Val using the BEST-TROSY-PRE experiment compared to the BEST-HSQC-PRE experiment. This variation in sensitivity between different regions of the sample is masked in Fig. 3A as the integral of all backbone amide peaks is dominated by strong signals from the more slowly relaxing disordered regions of the protein. At higher magnetic fields and/or for larger proteins, the favorability of the TROSY-based experiments compared to the HSQC-based experiments will be accentuated.

Relaxation times will be faster for amide protons close to the spin label when a sample is in the paramagnetic state. In our studies of intermolecular interactions[14] or longer-range interactions between different parts of an intrinsically disordered protein[26] the BEST sequences consistently resulted in better sensitivity because the PREs that we were interested in measuring were relatively small. However, for cases where very large PRE values are expected the BEST sequences (especially the sensitivity-enhanced versions) may prove less useful because of the large ^{1}H R_1 and R_2 values for the paramagnetic state.

One point of consideration when setting up PRE experiments is how many delay times should be used for measuring the relaxation rates. An analysis of this consideration carried out by Iwahara et al.[22] using synthetic data sets showed that, for a finite total experiment time, the precision of the resulting PRE values were slightly better if only two delay times were used. For example, if a spectroscopist only has enough spectrometer time to run a total of 1024 scans, they are theoretically better off measuring two delay times (with 512 scans each) rather than eight delay times (with 128 scans each). Another advantage of using two delay times is that the equations for calculating Γ_2 and the error in Γ_2 are straightforward to implement (equations 5 and 6 in Iwahara et al.[22]) and do not require fitting the peak intensities as a function of the delay time (Δ for the experiments shown in Fig. 1). However, the analysis by Iwahara and colleagues was for situations where it was assumed that all amide protons had approximately the same transverse relaxation rate in the diamagnetic state and only the rate in the paramagnetic state (and therefore the PRE) varied. For proteins that contain both structured and intrinsically disordered regions (like the IC-2$C_{1\text{-}96}$ sample used in this study), proton transverse relaxation rates can vary by an order of magnitude, so it is difficult to select a second delay time that is optimal for all resonances.

In practice, we prefer to collect data with a series of Δ values (typically eight values ranging from 0 to 30 ms), as shown in Fig. 2. This allows the decay curves in the pseudo-third dimension to be inspected for problems (which is particularly important when there is peak overlap) and also does not require as many assumptions about the range of ^{1}H R_2 values in the sample to select optimal Δ values. In addition, modern NMR software makes it easy to both visualize and to fit relaxation data. We use CCPN Analysis[18,27] for this task as it combines assignment and relaxation rate calculations in one package, but other software tools, such as Dynamics Center (Bruker BioSpin) or relax/relaxGUI[28], can be used instead.

Conclusions

The straightforward incorporation of the BEST methodology in pseudo-3D experiments for measuring ^{1}H R_2 values results in experiments that provide equally accurate measurements but with improved sensitivity. The BEST-HSQC-PRE and BEST-TROSY-PRE pulse sequences are available at:

https://webhost.lclark.edu/loening/pulses.shtml

Acknowledgements

We sincerely thank Frank Löhr (Goethe-Universität Frankfurt) for initially suggesting the BEST-TROSY-PRE sequence. Thanks to Elisar Barbar and Patrick Reardon (Oregon State University) for their advice and support. This work was supported by the National Science Foundation (Award 2003557). The Lewis & Clark College 600 MHz NMR spectrometer was purchased with support from the National Science Foundation (Award 1917696) and the M. J. Murdock Charitable Trust (Grant 201811283).

References:

1. Clore, G. M. & Iwahara, J. Theory, practice, and applications of paramagnetic relaxation enhancement for the characterization of transient low-population states of biological macromolecules and their complexes. *Chem. Rev.* **109**, 4108–4139 (2009).
2. Jensen, M. R., Ruigrok, R. W. H. & Blackledge, M. Describing intrinsically disordered proteins at atomic resolution by NMR. *Curr. Opin. Struct. Biol.* **23**, 426–435 (2013).
3. Kosol, S., Contreras-Martos, S., Cedeño, C. & Tompa, P. Structural characterization of intrinsically disordered proteins by NMR spectroscopy. *Molecules* **18**, 10802–10828 (2013).
4. Anthis, N. J. & Clore, G. M. Visualizing transient dark states by NMR spectroscopy. *Q. Rev. Biophys.* **48**, 35–116 (2015).
5. Clore, G. M. Practical aspects of paramagnetic relaxation enhancement in biological macromolecules. *Methods Enzymol.* **564**, 485–497 (2015).
6. Pervushin, K., Vögeli, B. & Eletsky, A. Longitudinal ^{1}H relaxation optimization in TROSY NMR spectroscopy. *J. Am. Chem. Soc.* **124**, 12898–12902 (2002).
7. Schanda, P., Kupce, E. & Brutscher, B. SOFAST-HMQC experiments for recording two-dimensional heteronuclear correlation spectra of proteins within a few seconds. *J. Biomol. NMR* **33**, 199–211 (2005).
8. Schanda, P. & Brutscher, B. Very fast two-dimensional NMR spectroscopy for real-time investigation of dynamic events in proteins on the time scale of seconds. *J. Am. Chem. Soc.* **127**, 8014–8015 (2005).
9. Schanda, P., Van Melckebeke, H. & Brutscher, B. Speeding up three-dimensional protein NMR experiments to a few minutes. *J. Am. Chem. Soc.* **128**, 9042–9043 (2006).
10. Lescop, E., Schanda, P. & Brutscher, B. A set of BEST triple-resonance experiments for time-optimized protein resonance assignment. *J. Magn. Reson. San Diego Calif 1997* **187**, 163–169 (2007).
11. Farjon, J. *et al.* Longitudinal-relaxation-enhanced NMR experiments for the study of nucleic acids in solution. *J. Am. Chem. Soc.* **131**, 8571–8577 (2009).
12. Lescop, E., Kern, T. & Brutscher, B. Guidelines for the use of band-selective radiofrequency pulses in hetero-nuclear NMR: example of longitudinal-relaxation-enhanced BEST-type ^{1}H-^{15}N correlation experiments. *J. Magn. Reson. San Diego Calif 1997* **203**, 190–198 (2010).
13. Favier, A. & Brutscher, B. Recovering lost magnetization: polarization enhancement in biomolecular NMR. *J. Biomol. NMR* **49**, 9–15 (2011).
14. Di Nicola, A. *et al.* Investigating binding between dynein intermediate chain and dynactin p150^{Glued}. *Protein Sci. Publ. Protein Soc.* **TBD**, (2025).
15. Jansson, M. *et al.* High-level production of uniformly ^{15}N- and ^{13}C-enriched fusion proteins in *Escherichia coli*. *J. Biomol. NMR* **7**, 131–141 (1996).

16. Davis, S. M., Romig, B. L., Abe, A. A. & Loening, N. M. An improved variant of tobacco etch virus (TEV) protease that does not need reducing agents. *Protein Sci. Publ. Protein Soc.* **34**, e70049 (2025).
17. Anthis, N. J. & Clore, G. M. Sequence-specific determination of protein and peptide concentrations by absorbance at 205 nm. *Protein Sci. Publ. Protein Soc.* **22**, 851–858 (2013).
18. Vranken, W. F. *et al.* The CCPN data model for NMR spectroscopy: development of a software pipeline. *Proteins* **59**, 687–696 (2005).
19. Donaldson, L. W. *et al.* Structural characterization of proteins with an attached ATCUN motif by paramagnetic relaxation enhancement NMR spectroscopy. *J. Am. Chem. Soc.* **123**, 9843–9847 (2001).
20. Palmer, A. G., Cavanagh, J., Wright, P. E. & Rance, M. Sensitivity improvement in proton-detected two-dimensional heteronuclear correlation NMR spectroscopy. *J. Magn. Reson. 1969* **93**, 151–170 (1991).
21. Kay, L. E., Keifer, P. & Saarinen, T. Pure absorption gradient enhanced heteronuclear single quantum correlation spectroscopy with improved sensitivity. *J. Am. Chem. Soc.* **114**, 10663–10665 (1992).
22. Iwahara, J., Tang, C. & Clore, G. M. Practical aspects of ^{1}H transverse paramagnetic relaxation enhancement measurements on macromolecules. *J. Magn. Reson. San Diego Calif 1997* **184**, 185–195 (2007).
23. Meiboom, S. & Gill, D. Modified Spin-Echo Method for Measuring Nuclear Relaxation Times. *Rev. Sci. Instrum.* **29**, 688–691 (1958).
24. Pervushin, K., Riek, R., Wider, G. & Wüthrich, K. Transverse relaxation-optimized spectroscopy (TROSY) for NMR studies of aromatic spin systems in ^{13}C-labeled proteins. *J. Am. Chem. Soc.* **120**, 6394–6400 (1998).
25. Meissner, A., Schulte-Herbrüggen, T., Briand, J. & Sørensen, O. W. Double spin-state-selective coherence transfer. Application for two-dimensional selection of multiplet components with long transverse relaxation times. *Mol. Phys.* **95**, 1137–1142 (1998).
26. Loening, N. M., Jara, K. A. & Barbar, E. J. NMR Approaches to Identify Transient Structure and Interactions of Intrinsically Disordered Dynein Intermediate Chain. *J. Mol. Biol.* 169380 (2025) doi:10.1016/j.jmb.2025.169380.
27. Skinner, S. P. *et al.* CcpNmr AnalysisAssign: a flexible platform for integrated NMR analysis. *J. Biomol. NMR* **66**, 111–124 (2016).
28. Bieri, M., d'Auvergne, E. J. & Gooley, P. R. relaxGUI: a new software for fast and simple NMR relaxation data analysis and calculation of ps-ns and μs motion of proteins. *J. Biomol. NMR* **50**, 147–155 (2011).